

Prediction of ferromagnetism in bcc Mn

J. L. Fry and Y. Z. Zhao

The University of Texas at Arlington, Arlington, Texas 76019

N. E. Brener, G. Fuster,* and J. Callaway

Louisiana State University, Baton Rouge, Louisiana 70803

(Received 13 April 1987; revised manuscript received 26 May 1987)

The many-body-enhanced magnetic susceptibility $\chi(q)$ has been computed for paramagnetic bcc Mn. An instability toward the formation of a ferromagnetic state at $T=0$ K is predicted and confirmed by spin-polarized band-structure and magnetic-moment calculations at several lattice constants. Strong ferromagnetism is predicted in a lattice-constant range larger than approximately 6.0 a.u.

I. INTRODUCTION

The transition metal Mn occurs in four allotropic forms, α , β , γ , and δ , at atmospheric pressure. The room-temperature form is complex body-centered cubic (bcc) with 29 atoms per primitive cell and becomes antiferromagnetic below 95 K. The γ phase is face-centered cubic (fcc) and occurs between 1364 and 1410 K, while the δ phase is bcc and occurs between 1410 and 1450 K, where it melts.^{1,2} Both γ and δ phases occur well above any expected magnetic order temperature but might be stabilized at lower temperatures by quenching, alloying, or epitaxial growth on cubic substrates.²⁻⁴ Previous studies have suggested that Mn is antiferromagnetic at low temperatures in the α , γ , and δ phases.^{1,2,5} This has been confirmed theoretically for γ -Mn by calculation of the enhanced susceptibility $\chi(q)$ for paramagnetic fcc Mn.⁶ To the contrary, however, $\chi(q)$ for bcc Mn presented below suggests that δ -Mn is ferromagnetic. This is supported by spin-polarized band-structure calculations at several lattice constants.

II. MAGNETIC SUSCEPTIBILITY OF PARAMAGNETIC δ -Mn

Expressions for the many-body-enhanced susceptibility, $\chi(q)$, within a local-orbital, local-density approximation are given by Callaway and co-workers:^{7,8}

$$\chi_{st}(\mathbf{q}, \omega) = \sum_{i,j,l,m} I_{ij}(\mathbf{q}_s) \Gamma_{ij,lm} I_{lm}(-\mathbf{q}_t),$$

where $\Gamma_{ij,lm}$ is the enhanced wave-vector- and frequency-dependent susceptibility on an orbital basis and $I_{ij}(\mathbf{q})$ is an atomic form factor.

$$\Gamma_{ij,i'j'} = \sum_{l,m} \gamma_{ij,lm} [(I - X)^{-1}]_{lm,i'j'}, \quad (2)$$

and

$$X_{ij,i'j'} = \sum_{s,t,l,m} I_{ij}(-\mathbf{p}_s) \Lambda(\mathbf{K}_s - \mathbf{K}_t) I_{lm}(\mathbf{p}_t) \gamma_{lm,i'j'}. \quad (3)$$

Here Λ is a matrix in reciprocal-lattice vectors \mathbf{K}_s and \mathbf{K}_t , related to the local exchange-correlation potential of the

band-structure calculation. The matrices Λ , γ , and I are defined in Ref. 8.

Since calculation with these equations is very time consuming we employed the two-centered, orthogonal Slater-Koster band structure of Papaconstantopoulos.⁹ Matrix elements I_{ij} were computed using the procedure of Ref. 8, except wave functions were generated from the self-consistent, muffin-tin potentials of Moruzzi, Janak, and Williams.¹⁰ The matrix Λ was computed with the von Barth-Hedin exchange-correlation potential¹¹ and the charge densities of Ref. 10. We did not make the diagonal approximation of Ref. 9, but were able to keep all terms by using a modification of the analytic tetrahedron method¹² (ATM) to do the time-consuming calculation of γ . While approximations discussed in the references above were necessary, we introduced no adjustable parameters. The random-phase approximation (RPA) $\chi_0(q)$ and $\chi(q)$ for paramagnetic bcc Mn are shown along a cubic axis in Fig. 1. The negative value of $\chi(0)$ of our

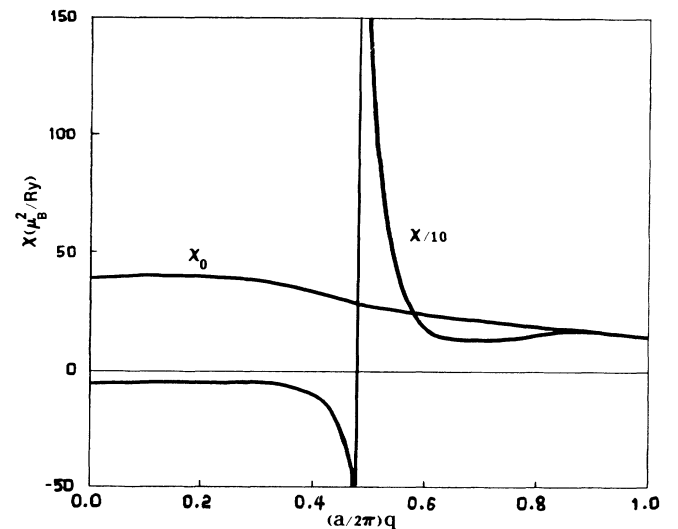


FIG. 1. RPA χ_0 and enhanced susceptibility χ for bcc Mn along a cubic axis. χ has been divided by 10 to reveal structure of χ_0 .

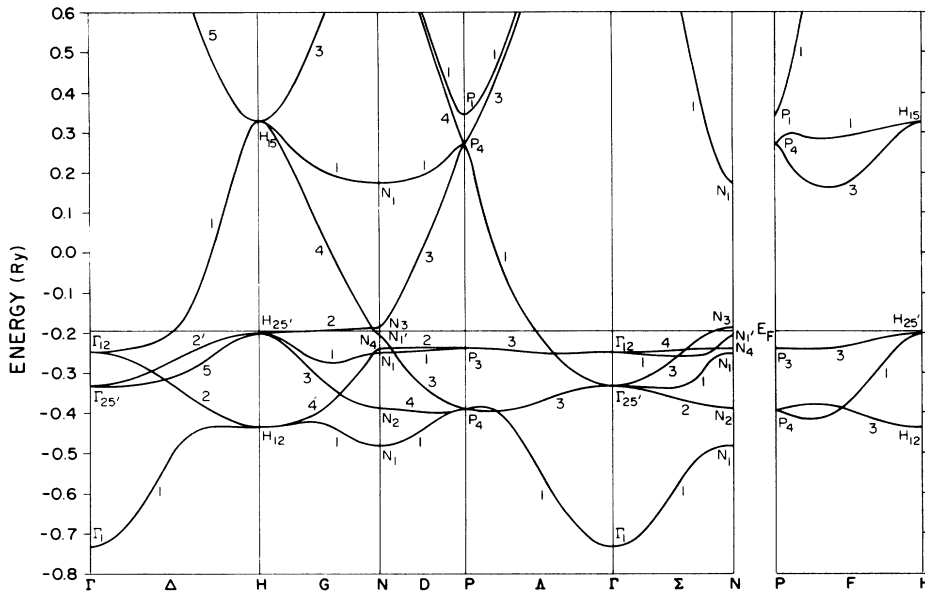


FIG. 2. Majority-spin band structure for ferromagnetic bcc Mn at lattice constant $a = 6.0$ a.u.

enhanced susceptibility at $q = 0$ predicts ferromagnetism. This agrees with predictions that are made using our $\chi_0(0)$ and Janak's¹³ enhancement method with his parameter I : bcc Mn should be ferromagnetic at low temperature.

III. BAND STRUCTURE AND MAGNETIC MOMENT

We have used the linear combination of Gaussian orbitals (LCGO) method to perform a local-density, spin-polarized, all-electron calculation of the band structure of

bcc manganese. We employed the program BNDPKG,¹⁴ which had been used previously by Wang and Callaway to compute the energy bands of ferromagnetic nickel and iron.^{15,16} The von Barth-Hedin¹¹ form of the spin-polarized, local-density exchange-correlation potential, as parametrized by Rajagopal, Singhal, and Kimball¹⁷ was used in the present calculation.

We employed the Wachters¹⁸ basis set for Mn, consisting of 13 s , 10 p , and 5 d primitive Gaussians, plus a single f orbital. All of the primitive Gaussians were treated as individual functions (no contractions), giving a total of 75 basis functions. The energy-band and magnetic-moment

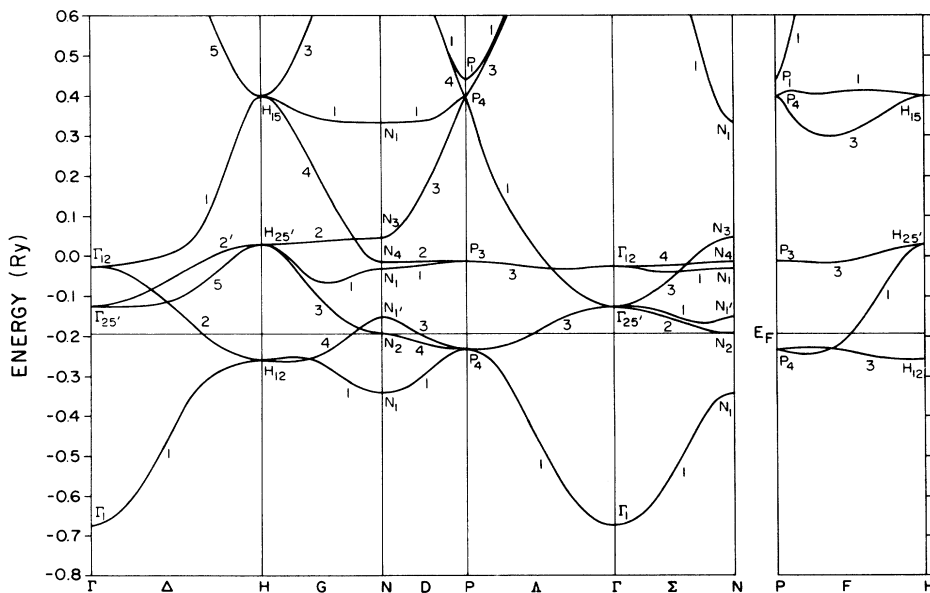


FIG. 3. Minority-spin band structure for ferromagnetic bcc Mn at lattice constant $a = 6.0$ a.u.

calculations were done for a number of different lattice constants. The band structure shown in Figs. 2 and 3 was done for a lattice constant of 6.0 a.u. A self-consistency convergence criterion of $10^{-4} \mu_B$ for the magnetic moment was used in the band calculations. The iterated potential was computed using 55 points in the irreducible part of the Brillouin zone (IBZ). The final band structure was generated at 506 points in the IBZ.

The Fermi surface for ferromagnetic Mn is complicated and changes shape rapidly with lattice constant near $a=6$ a.u. as the majority-spin $3d$ bands fill and s bands begin to split. Approximate spin splittings at $a=5.80$, 6.00 , and 8.00 a.u. are, respectively, 0.0 , 0.7 , and 1.0 eV for s bands and 1.0 , 3.0 , and 4.0 eV for d bands. As a consequence of the rapid change in spin splitting near $a=6$ a.u. an abrupt transition from low-spin to high-spin ferromagnetism occurs as the Fermi energy moves through the top, almost flat, majority-spin, d band (Fig. 2).

Table I gives the computed magnetic moment of bcc Mn at a number of lattice constants ranging from 5.2 a.u. (the computed paramagnetic equilibrium value¹⁹) to 8 a.u., where the magnetic moment is near the maximum value for an isolated Mn atom. Figure 4 shows the abrupt increase which occurs near $a=6.0$ a.u. at the low-spin to high-spin transition.

The magnetization (magnetic moment per unit volume) as a function of lattice constant is also given in Table I and plotted in Fig. 5. In order to emphasize the strength of the high-spin magnetization of bcc Mn, it is expressed in terms of the equilibrium magnetization of bcc Fe, which was computed using a magnetic moment of $2.12 \mu_B$ and lattice constant of 5.40 a.u. (Ref. 20). The sharp increase provides a range of lattice constants from 5.95–6.70 a.u. for which the magnetization of bcc Mn exceeds that of bcc Fe at equilibrium by as much as 20%.

The lattice constant at the transition is close enough to the paramagnetic equilibrium lattice constant, and the expected (but not yet computed) ferromagnetic equilibrium lattice constant, that there is some hope of growing the

TABLE I. Lattice constant a , and magnetic moment m , and relative magnetization M^{rel} , for bcc Mn. M^{rel} is defined as the magnetization of Mn divided by the magnetization of bcc Fe at its equilibrium value.

a (a.u.)	m (μ_B)	M^{rel}
5.200	0.76	0.401
5.397	0.93	0.439
5.450	0.97	0.445
5.628	1.09	0.454
5.800	1.18	0.449
5.900	1.24	0.448
5.925	1.26	0.450
5.950	3.12	1.100
5.975	3.40	1.184
6.000	3.49	1.200
6.025	3.53	1.199
6.050	3.56	1.194
7.000	4.37	0.946
8.000	4.93	0.715

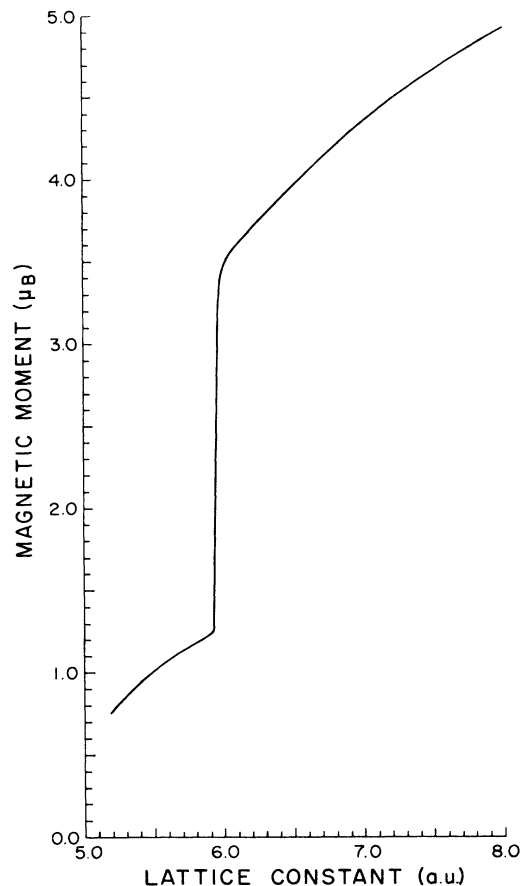


FIG. 4. Magnetic moment of bcc Mn vs lattice constant.

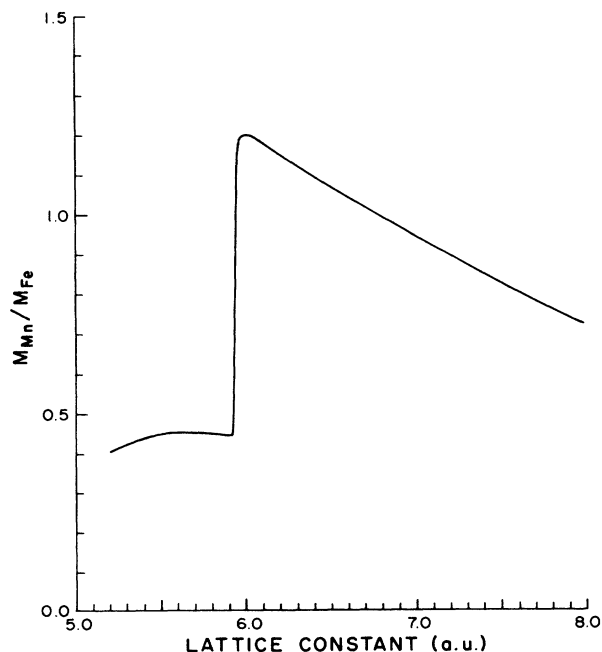


FIG. 5. Magnetization of bcc Mn relative to the equilibrium magnetization of bcc Fe.

high-spin phase of bcc Mn as an epitaxial film on another bcc substrate with the desired lattice constant. An interesting set of bcc substrates would be Mo, W, Nb, and Ta with lattice constants of 5.95, 5.98, 6.24, and 6.25 a.u., respectively.

While our spin-polarized LCGO calculations predict ferromagnetism at all lattice constants in Fig. 4, it should be noted that the BNDPKG program used here does not permit consideration of a possible antiferromagnetic state. Hence the band calculation cannot lead to a prediction as to whether bcc Mn might be antiferromagnetic instead of ferromagnetic. It is the susceptibility calculation which indicates that the dominant instability should be toward ferromagnetism.

IV. CONCLUSION

We have made what we believe to be the first prediction of a ferromagnetic low-temperature state for δ -Mn. Fer-

romagnetism is predicted at all lattice constants considered and strong ferromagnetism for $a > 6$ a.u. The predictions are based upon a ferromagnetic instability of the linear response of the paramagnetic bcc phase and are confirmed by our spin-polarized LCGO band calculations. Whether other magnetic states of δ -Mn are possible (or preferred energetically) must be determined by total-energy calculations²¹ or by experiments.^{3,4} We certainly have enough evidence to stimulate such work for Mn.

ACKNOWLEDGMENTS

Research at the University of Texas at Arlington was supported by the Robert A. Welch Foundation and by the Air Force Office of Scientific Research Grant No. AFOSR-83-0050. Work at Louisiana State University was supported in part by the National Science Foundation under Grant No. DMR-8504259.

*Permanent address: Universidad Santa Maria, Valparaiso, Chile.

¹R. J. Weiss and K. J. Tauer, *J. Phys. Chem. Solids* **4**, 135 (1958).

²A. Arrott, in *Magnetism*, edited by G. T. Rado and H. Suhl (Academic, New York, 1966), Vol. IIB, Chap. 4.

³A. Arrott, *Bull. Am. Phys. Soc.* **32**, 707 (1987).

⁴bcc cobalt has been prepared: G. A. Prinz, *Phys. Rev. Lett.* **54**, 1051 (1985).

⁵S. Asano and J. Yamashita, *Prog. Theor. Phys.* **49**, 373 (1973); *J. Phys. Soc. Jpn.* **31**, 1000 (1971).

⁶Y. Z. Zhao, J. L. Fry, P. C. Pattnaik, and K. Schwartzman (unpublished).

⁷J. Callaway and A. K. Chatterjee, *J. Phys. F* **8**, 2569 (1978).

⁸J. Callaway, A. K. Chatterjee, S. P. Singhal, and A. Ziegler, *Phys. Rev. B* **28**, 3818 (1983).

⁹D. A. Papaconstantopoulos, *Handbook of the Band Structure of Elemental Solids* (Plenum, New York, 1986).

¹⁰V. L. Moruzzi, J. F. Janak, and A. R. Williams, *Calculated Electronic Properties of Metals* (Pergamon, New York, 1978).

¹¹U. von Barth and L. Hedin, *J. Phys. C* **5**, 1629 (1972).

¹²J. Rath and A. J. Freeman, *Phys. Rev. B* **11**, 2109 (1975).

¹³J. F. Janak, *Phys. Rev. B* **16**, 255 (1977).

¹⁴C. S. Wang and J. Callaway, *Comput. Phys. Commun.* **14**, 327 (1978).

¹⁵C. S. Wang and J. Callaway, *Phys. Rev. B* **15**, 298 (1977).

¹⁶J. Callaway and C. S. Wang, *Phys. Rev. B* **16**, 2095 (1977).

¹⁷A. K. Rajagopal, S. P. Singhal, and J. Kimball, *Adv. Chem. Phys.* **41**, 59 (1979).

¹⁸A. J. H. Wachters, *J. Chem. Phys.* **52**, 1033 (1970).

¹⁹D. A. Papaconstantopoulos (private communication).

²⁰H. Danan, A. Herr, and A. J. P. Meyer, *J. Appl. Phys.* **39**, 669 (1968).

²¹V. L. Moruzzi, P. M. Marcus, K. Schwarz, and P. Mohn, *Phys. Rev. B* **34**, 1784 (1986).